Title
Groundstate properties of YbBiPt

Journal
Physica B Condensed Matter, 197(1-4)

ISSN
0921-4526

Authors
Canfield, PC
Movshovich, R
Robinson, RA
et al.

Publication Date
1994-03-01

DOI
10.1016/0921-4526(94)90203-8

ELSEVIER

Physica B 197 (1994) 101–108

PHYSICA B

Groundstate properties of YbBiPt

P.C. Canfield[a,*], R. Movshovich[b], R.A. Robinson[b], J.D. Thompson[b], Z. Fisk[b], W.P. Beyermann[c], A. Lacerda[d], M.F. Hundley[b], R.H. Heffner[b], D.E. MacLaughlin[c], F. Trouw[e], H.R. Ott[f]

[a]*Ames Lab and Iowa State University, Ames, IA 50011, USA*
[b]*Los Alamos National Laboratory, Los Alamos, NM 87545, USA*
[c]*University of California, Riverside, CA 92521, USA*
[d]*National High Magnetic Field Laboratory, Los Alamos, NM 87545, USA*
[e]*Argonne National Laboratory, Argonne, IL 60439, USA*
[f]*Laboratorium für Festkörperphysik, ETH, Zürich, Switzerland*

Abstract

The physical properties of YbBiPt are complicated because there are three competing energy scales all of order 1 K: the coupling energy between Yb moments as measured by the Néel temperature (T_N), the splitting between the groundstate and first excited crystal electric field levels ($T_{\Delta CEF}$) and the Kondo temperature (T_K). The magnetically ordered phase below $T_N = 0.45$ K appears to be reduced local moment ordering that is incommensurate with the lattice. Associated with this order is the formation of a superzone gap that can be detected by electrical resistivity measurements. Attempts to treat T_K and $T_{\Delta CEF}$ separately only account for gross features of the data presented.

1. Introduction

The discovery of a linear contribution to the low-temperature specific heat in excess of 8 J/mol K^2 in YbBiPt [1] has caused great interest in this last magnetic member of the RBiPt series [2] (R = rare earth). Although a substantial body of data from diverse measurements has formed [3–9], a unified picture of the groundstate has not emerged.

Examination of this body of data does, however, reveal several salient energy scales. There is a phase transition at 0.45 K that is magnetic in origin [3,7,9] and has a magnetic susceptibility consistent with antiferromagnetism [1,2,6]. In addition, the size of the ordered moment detected by μSR measurements is $0.1\mu_B$ [3,7,9], which is consistent with the lack of a nuclear Schottky anomaly in the low-temperature specific heat [1,6]. The size of the ordered moment, the magnitude of the low-temperature linear specific heat and the small integrated entropy through $T = 0.45$ K raise the question: to what degree is Kondo-like screening of the Yb moments playing a role in the ground state? In addition the question of the size of crystal electric field (CEF) splittings must also be addressed, since large values of specific heat can also arise from atomic Schottky-like anomalies

* Corresponding author.

SSDI: 0921-4526(93)E0166-E

associated with small CEF splittings. In order to better understand the groundstate of YbBiPt we will examine the three, competing, low-temperature energy scales all of which are of order 1 K: the coupling strength between Yb moments as manifest by the Néel temperature (T_N), the energy difference between the ground and first excited CEF levels ($T_{\Delta CEF}$), and the Kondo temperature (T_K). Unraveling different aspects of experimental data that can be associated with each of these energy scales is the challenge that YbBiPt currently poses.

This paper will focus on what has been learned about the low-temperature properties of YbBiPt. In particular it will examine aspects of the experimental data that we think can be primarily associated with each of these three energy scales. Of course, it will quickly be evident that such a segregation is artificial, but the conceptual convenience that it offers is of value as long as it does not misrepresent the data. We will first examine data associated with the antiferromagnetic transition at $T_N = 0.45$ K. This will lead to a discussion of the CEF splitting in YbBiPt. Finally the effects of Kondo screening will be examined. The goal is to present our current thinking about YbBiPt and point out what we feel are some of the salient, unanswered questions associated with this material.

2. Experimental methods

All of the data presented are from measurements preformed on single crystals (or collections of single crystals) of YbBiPt grown from excess Bi flux [10]. Due to slight surface contamination of the crystals by a BiPt film that superconducts below 1 K, transport measurements, such as temperature-dependent electrical resistance and magnetoresistance, were performed on crystals that were polished to remove the outer surfaces that suffer from this contamination.

Electrical resistivity measurements were performed on samples by a standard four-probe AC technique. Initially, rod-shaped samples were used to measure resistivity along one specific crystallographic direction. Later platelets were used to simultaneously measure the resistivity along two orthogonal directions via the Montgomery method [11]. Specific heat measurements were performed by a variation of a semi-adiabatic method in a dilution refrigerator between 1.2 K and 100 mK. Above 1.2 K a thermal relaxation technique was used. The neutron scattering data presented here were collected at the QENS spectrometer at Argonne National Laboratory [12].

One point that should be kept in mind when comparing specific heat, electrical resistivity and magnetic susceptibility results to neutron scattering (or μSR) results is that the former measurements generally use only one or two single crystals, while the latter use collections of thousands. This can lead to slight variations in results since a single crystal chosen from thousands will usually be one of the better formed, cleaner ones. In addition, the neutron scattering and μSR results will be averaging over thousands of separate crystals, while the transport and thermodynamic measurements will be more sensitive to sample-to-sample variation.

3. Experimental results and analysis

Figure 1(a) shows the electrical resistivity for three samples of YbBiPt at low temperatures with the current flowing along directions solely determined by the growth habit of each sample. The anomaly seen at 0.45 K is associated with the specific heat anomaly seen at the same temperature in Fig. 2. Magnetic susceptibility [1,6] and μSR measurements [3,7,9] have identified this transition as antiferromagnetic in nature and give an ordered moment of approximately $0.1\mu_B$. To further investigate the nature of the anomaly and to determine whether the variations seen in Fig. 1(a) are intrinsic or extrinsic to the material, we measured a sample that was polished from a (1 0 0) face of a single crystal in a Montgomery configuration [11]. The results of this measurement are shown in Fig. 1(b). The onset of anisotropy seen at the transition temperature indicates that there is a break-

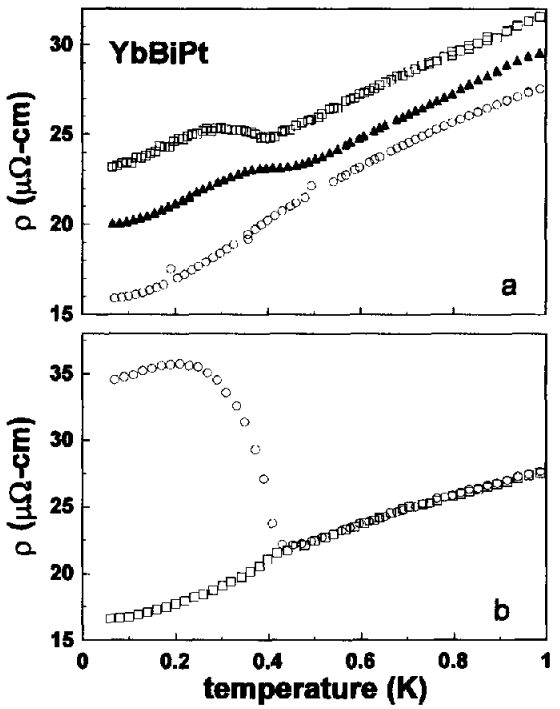

Fig. 1. (a) Resistivity vs temperature for three samples of YbBiPt. For clarity the solid triangles are shifted by 2 μΩ cm and the open squares by 4 μΩ cm. (b) Resistivity vs temperature for a single sample of YbBiPt measured in the Montgomery configuration.

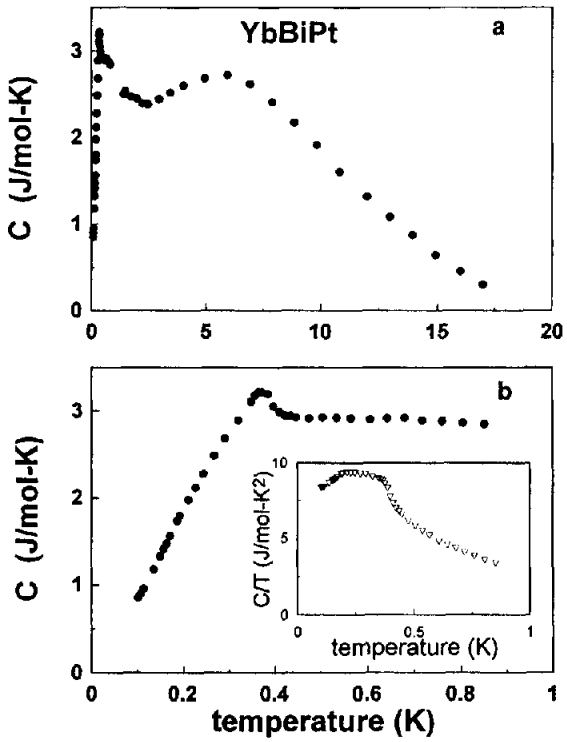

Fig. 2. Magnetic contribution to the specific heat of YbBiPt vs temperature [C(YbBiPt) − C(LuBiPt)]. (a) 0 K to 20 K, (b) 0 K to 1 K. Inset: magnetic specific heat divided by temperature vs temperature.

ing of the cubic symmetry of this material. The possible origins of this symmetry breaking will be discussed later, but its existence implies that the variety of resistance curves seen in Fig. 1(a) is intrinsic to YbBiPt.

The resistive anomaly seen in YbBiPt at 0.45 K is qualitatively similar to those seen in other members of the RBiPt series [2]. Figure 3(a) shows data for GdBiPt and Figs. 3(b) and 3(c) shows data for TbBiPt and DyBiPt respectively. The discontinuous nature of the magnetic transition seen at T_N in the resistance of DyBiPt is not observed in specific heat data which are consistent with a second-order phase transition. It should be noted that, while GdBiPt has an integrated magnetic entropy up to T_N consistent with ordering of the full $J = 7/2$ multiplet, DyBiPt and TbBiPt have integrated magnetic entropies of approximately 8.5 J/mole K (75% R ln 4) [2], indicating the existence of CEF levels above the ordering temperature that lower the ground state degeneracy.

There currently seem to be three possible origins of the resistive anomaly that accompanies the transition to the antiferromagnetic ground-state: (i) localized moments order and a super-zone gap emerges as a result of the magnetically imposed periodicity, (ii) a spin density wave (SDW) forms out of the conduction band, also leading to a partial gapping of the Fermi surface, or (iii) there is a cooperative Jahn–Teller effect accompanying the magnetic order of localized moments that leads to a distortion of the lattice to tetragonal or lower symmetry. The first two of these possibilities are Fermi surface effects while the third is more directly related to the nature of the CEF splitting of the material, but in all cases there is a breaking of the high-temperature, cubic symmetry.

The fundamental difference between a SDW

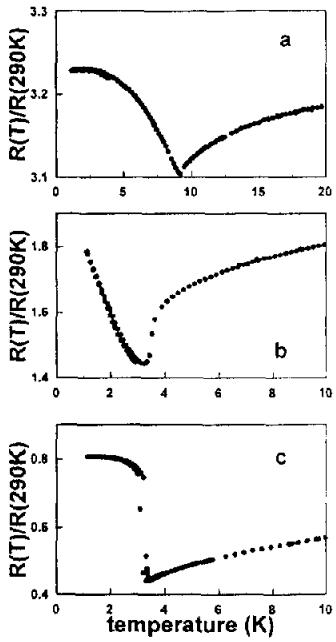

Fig. 3. Normalized resistance vs temperature for (a) GdBiPt, (b) TbBiPt and (c) DyBiPt.

and superzone gap is the nature of the ordered moments, whether there are localized moments on the Yb sites just above T_N or not. In each case the nesting of the Fermi surface determines the ordering wavevector of the antiferromagnetic ground state. In the case of a superzone gap, nesting of the Fermi surface determines the ordering wave vector of the localized moments [13]. In the case of a SDW the nesting of the Fermi surface gives rise to a periodic modulation of the conduction electron spin density, i.e. under proper conditions (sufficiently strong electron–electron interaction and large enough areas of the Fermi surface nesting), the nesting not only determines the ordering wave vector, but also gives rise to the ordered moments [14]. Unfortunately, resistivity measurements are sensitive to the actual loss of Fermi surface and not the cause of the loss and therefore cannot distinguish between these two magnetically ordered groundstates. μSR data indicates that there is magnetic order below T_N that is incommensurate with the lattice [7,9]. This also is consistent with either a SDW or the type of local moment ordering that could give rise to a superzone gap.

Examination of other members of the RBiPt series leads to some clues about the origin of the Fermi surface effect seen at T_N. Anomalies in the resistance similar to what is found in YbBiPt are found at T_N in GdBiPt, DyBiPt and TbBiPt. These features are similar to those in the elemental rare earths when there is the formation of superzone gaps associated with magnetic order. Since no anomalies are seen in the resistivities or susceptibilities of either YBiPt or LuBiPt that can be associated with the formation of a SDW state, it seems clear that the Fermi-surface effect in GdBiPt, TbBiPt and DyBiPt is driven by ordering of localized moments and is associated with the formation of a superzone gap. It is therefore likely that the anomaly in YbBiPt can also be described as a superzone gap.

The one conspicuous problem with invoking a Fermi surface effect is that it presupposes the existence of an occupied conduction band. In these materials there is an increasingly semiconductive behavior as the rare earth progresses from Yb to Nd [2]. In NdBiPt the resistivity increases by 700% on cooling from 300 K down to 2 K and in GdBiPt the resistance increases by 250%. It is possible that there is nesting in the small pockets of Fermi surface that make up such a semi-metal (similar to the nesting seen in the small pockets of the Cr Fermi surface [15]), but the semi-metallic nature of the series does raise questions of the appropriateness of invoking Fermi-surface effects, particularly for the lighter rare earth members of the series. In YbBiPt, on the other hand, the existence of an occupied conduction band is not an issue. The temperature dependent resistivity is monotonically increasing [2] with increasing temperature from 2 K to 300 K. In addition, the Kondo screening of the Yb moments requires a finite density of states at the Fermi surface and recent band structure calculations [16] as well as Hall effect measurements [17] indicate that there are small hole-like pockets at the Fermi surface.

Another possible contribution to the resistive anomalies seen in the RBiPt series is that a

cooperative Jahn–Teller effect accompanies the antiferromagnetic transitions [18]. This would be similar to the transitions seen in members of the closely related structures RBi and RSb [18,19]. In CeSb, for example, there is an antiferromagnetic transition at 16 K that is accompanied by a cubic-to-tetragonal distortion [20] which splits the Γ_8 CEF level of Ce. A requirement for this transition is that there be a non-Kramers CEF level that has nonzero quadrupole matrix elements either at or near the ground state level. In the case of YbBiPt it seems likely that the Γ_8 quartet meets this requirement. The distortion that accompanies this transition could be partially responsible for the anisotropy seen in the resistance data below T_N. An advantage of this mechanism is that it does not depend on the existence of conduction electrons, and therefore is perfectly acceptable for a semi-metallic or even insulating materials. A cooperative Jahn–Teller effect could then be part of the phase transition observed in members of the RBiPt series that have a non-Kramers CEF level as or near the ground state.

One point that none of these models addresses is why do samples of YbBiPt form large or single domains in the low temperature groundstate? if the domains were small and randomly oriented, all of the curves in Fig. 1 would fall on top of each other due to averaging. Since there is a significant anisotropy seen in Fig. 1(b), there must be a preferential orientation of domains in the sample [15,21]. This is also borne out by the variation of low-temperature resistance curves shown in Fig. 1(a). The most probable mechanism for such a preferential seeding of domains is residual strain in the crystal. This strain may be left over from the growth process, induced during the polishing, or induced by thermal contraction. Whichever way the strain is created, it is likely that only a very small strain is necessary to induce preferred orientation. In both the case of a SDW transition (such as seen in Cr [15,22]) or cooperative Jahn–Teller transition [18–20] small strains can cause the formation of single domain samples. The pressure sensitivity of YbBiPt has been dramatically demonstrated in recent measurements of the hydrostatic pressure dependence of T_N. The resistive anomaly is suppressed to below 30 mK by an applied pressure of 0.7 ± 0.2 kbar [8]. Such a large pressure dependence for such a small transition temperature is consistent with the idea of small residual strains seeding domains preferentially [23]. In addition to being strain sensitive, domain formation in YbBiPt is likely to be highly magnetic-field-sensitive. If we use Cr as an example [15], we see that application of a 3 T field while cooling through the SDW transition at 311 K can lead to single domain samples. If we scale this to a transition temperature of 0.45 K, we then estimate that applied fields of millitesla could lead to single domains samples too. The effects of externally applied strain or magnetic fields on domain formation have not yet been examined.

The nature of the CEF splitting in this compound is currently a topic of some debate. The specific heat data shown in Fig. 2(a) does set some boundary conditions on the nature of the CEF splitting scheme. Since the integrated magnetic entropy is approximately $R \ln 5$ up to 20 K, there have to be doublet (Γ_6 or Γ_7) and a quartet (Γ_8) below that temperature and one doublet significantly above. In addition, the feature seen in Fig. 2(a) at approximately 6 K would be consistent with Schottky anomaly from a CEF level at approximately 12 K [24]. A better fit to the magnitude of the specific heat data comes from a Γ_8 ground state with one of the doublets at 12 K, but the reverse cannot be conclusively ruled out [25]. The question that then remains is: can the order of the CEF levels, and the splittings between them be determined more quantitatively? A further examination of the data sheds some light on this issue, but raises more questions than it answers.

The results of inelastic neutron scattering on YbBiPt at $T = 10$ K are shown in Fig. 4. At first glance, these data seem to be in good agreement with the interpretation of the specific heat data shown in Fig. 2(a). A closer analysis, though, reveals two distinguishable quasi-elastic features along with a separate excitation at 5.8 meV [5,26]. All of these features are significantly broader than the intrinsic 70 μeV resolution of

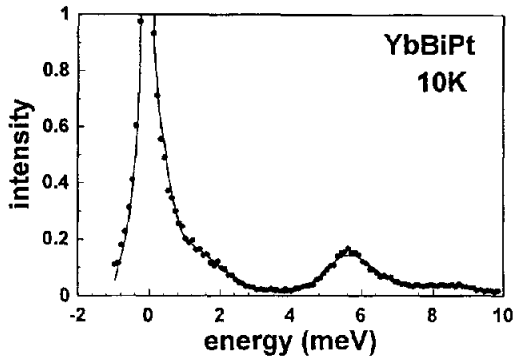

Fig. 4. Neutron-scattering intensity as a function of energy transfer for YbBiPt at 10 K. The points represent the data and the line is a fit assuming gaussian functions for each element of the two-component quasi-elastic response, the 5.8 meV excitation and the tail at 8 meV, following the treatment in Ref. [5].

the spectrometer [12]. The two quasi-elastic peaks are interpreted as the quartet and a doublet that are nearly degenerate. The splitting between these levels is estimated to be roughly 1 K [5,26]. This then leaves the 5.8 meV excitation to be the final doublet since both the temperature dependence and Q-dependence of this excitation are consistent with a CEF level and inconsistent with scattering by phonons [5,26]. The CEF splitting scheme from this analysis is then a doublet and the Γ_8 quartet split by only 1 K and the final doublet at 5.8 meV. The width of the ground state doublet is 2 K and the widths of the Γ_8 and the 5.8 meV doublet are both 10 K [5,26]. Such a scheme will not give a feature at 6 K in the specific heat, but it does yield a qualitative fit to the specific heat data with an integrated entropy of $R \ln 5$ by 11 K and $C/T = 10\,\mathrm{J/mol\,K^2}$ at 0.5 K [26]. While there is qualitative agreement between the models based upon the neutron scattering results and the specific heat data, there is still some disagreement regarding the details. Specifically, the CEF level at 5.8 meV provides more entropy than is observed by 20 K. In addition, the CEF splitting scheme and widths found by neutron scattering do not give the reduced high-temperature moment of $4.2\mu_B$ found in magnetic susceptibility measurements [1].

The primary question that has to be addressed in trying to understand the CEF levels in YbBiPt is whether the whole CEF splitting terminology is even appropriate. Strictly speaking CEF splitting terminology was developed for the point charge model [27]. In the case of YbBiPt the assumption of a point charge model is questionable because, as will be noted below, the Kondo temperature may be comparable to the first CEF splitting. This makes YbBiPt similar to uranium compounds, where the question of the CEF terminology has also been debated [28,29]. Whether the apparent discrepancies between the neutron scattering data and the specific heat data are real or an artifact of the inappropriate use of the CEF terminology remains to be seen.

This then leads us to the final temperature scale associated with this problem, the Kondo temperature. This energy scale is the least well defined of the three. To some extent it is inferred more than it is directly measured. Deviations from the predictions of the simple CEF splitting models for the magnetic susceptibility and specific heat are likely to be partly due to the existence of Kondo screening of the localized moments, but the exact Kondo temperature is hard to determine. If the full value of the $T \rightarrow 0$ K electronic specific heat is a consequence of the renormalized electron mass, then the Kondo temperature would be of the order of 1 K [1]. If some of that specific heat were attributed to Schottky contributions, then the Kondo temperature could be higher by factors of two or three. One way of defining the Kondo temperature is as the half-width of the quasi-elastic neutron scattering response, which is normally taken to be a well-defined single Lorentzian. In the case of YbBiPt, the quasi-elastic response is more complicated. If the two components of the quasi-elastic lineshape have well-defined, albeit different, widths due to different hybridizations of the CEF levels with the conduction band, then the groundstate doublet has a T_K of 2 K and the quartet has a T_K of 10 K. The Kondo temperature that is seen in thermodynamic or transport measurements may be a weighted average of these two values.

Although the precise value of the Kondo temperature is hard to determine, the existence

of Kondo-like spin compensation can be deduced by the reduced ordered moment of $0.1\mu_B$ seen in the low-temperature antiferromagnetic groundstate. This value is well below the effective moment associated with any of the CEF levels. Low-temperature Kondo screening is also consistent with a greatly enhanced linear specific heat coefficient and could help explain the complex form of the whole low-temperature specific heat curve.

Other measurements that traditionally have been used to examine the groundstate of Kondo lattices are complicated by the small CEF splittings. The magnetic field dependence of the low-temperature resistance and specific heat will be mixtures of Kondo-like effects and CEF effects when the applied field is of comparable magnitude to the CEF splittings. Once this happens a mixing (further mixing) of the CEF levels can lead to large field dependent effects. This mixing of the Kondo-like and CEF effects is simply a manifestation of the fact that both effects build off of the magnetic groundstate of Yb. This, then, signals the breakdown of the artificial separation of the three energy scales which, at this point, becomes a hindrance. The details of the specific heat and neutron scattering data, as well as magnetic field dependent effects, will only be fully accounted for by an analysis that treats all three of these energies simultaneously.

4. Conclusions

The phase transition observed in YbBiPt at $T_N = 0.45$ K gives rise to an anisotropic anomaly in the resistivity that can be associated with some combination of the formation of either a SDW or a superzone gap and a cooperative Jahn–Teller distortion. The anisotropy associated with this transition can only manifest itself if there is a preferential orientation of domains in the low-temperature state. Such a preferential orientation is thought to arise from the highly strain-sensitive nature of the transition.

The CEF effects seen in neutron scattering measurements are consistent with placing the Γ_8 quartet and a doublet below 20 K and the other doublet at 60 K. This CEF scheme is in rough agreement with the specific heat measurements performed below 20 K. Analysis of the specific heat data gives $T_{\Delta CEF} \simeq 10$ K while analysis of the neutron scattering data give $T_{\Delta CEF} \simeq 1$ K. The exact splitting, broadening and overlap of the CEF levels is not clear. For that matter, the whole language of well-defined CEF levels at low temperatures may not even be appropriate for this material.

The existence of a Kondo temperature is not in doubt, since the ordered moment of $0.1\mu_B$ in the antiferromagnetic ground state is much lower than the moment associated with any of the CEF levels. The size of the Kondo temperature cannot be unambiguously determined although analysis of the data presented here indicates that $1\text{ K} \leq T_K \leq 10\text{ K}$. The percentage of the low-temperature specific heat associated with the correlated electronic ground state versus the percentage associated with CEF or other effects is not known either.

Acknowledgements

Ames Laboratory is operated for the United States Department of Energy by Iowa State University under Contract No. W-7405-Eng-82. This work was supported by the Director for Basic Energy Research, Office of Basic Energy Science. Work performed at Los Alamos National Laboratory was done under the auspices of the United States Department of Energy.

References

[1] Z. Fisk, P.C. Canfield, W.P. Beyermann, J.D. Thompson, M.F. Hundley, H.R. Ott, E. Felder, M.B. Maple, M.A. Lopez de la Torre, P. Visani and C.L. Seaman, Phys. Rev. Lett. 23 (1991) 3310.

[2] P.C. Canfield, J.D. Thompson, W.P. Beyermann, A. Lacerda, M.F. Hundley, E. Peterson, Z. Fisk and H.R. Ott, J. Appl. Phys. 70 (1991) 5800.

[3] A. Amato, P.C. Canfield, R. Feyerherm, Z. Fisk, F.N. Gygax, R.H. Heffner, D.E. MacLaughlin, H.R. Ott, A. Schenck and J.D. Thompson, Phys. Rev. B 46 (1992) 3151.

[4] A. Lacerda, R. Movshovich, M.F. Hundley, P.C. Canfield, D. Arms, G. Sparn, J.D. Thompson, Z. Fisk, R.A. Fisher, N.E. Phillips and H.R. Ott, J. Appl. Phys. 73 (1993) 5415.
[5] R.A. Robinson, M. Kohgi, T. Osakabe, P.C. Canfield, T. Kamiyama, T. Nakane, Z. Fisk and J.D. Thompson, Physica B 186–188 (1993) 550.
[6] J.D. Thompson, P.C. Canfield, A. Lacerda, M.F. Hundley, Z. Fisk, H.R. Ott, E. Felder, M. Chernikov, M.B. Maple, P. Visani, C.L. Seaman, M.A. de la Torre and G. Aeppli, Physica B 186–188 (1993) 355.
[7] A. Amato, P.C. Canfield, R. Feyerherm, Z. Fisk, F.N. Gygax, R.H. Heffner, E.A. Knetsch, D.E. MacLaughlin, H.R. Ott, A. Schenck, J.D. Thompson and U. Zimmermann, Physica B 186–188 (1993) 615.
[8] R. Movshovich, A. Lacerda, P.C. Canfield, D. Arms, J.D. Thompson and Z. Fisk, in: Proceedings of the International Conference on Strongly Correlated Electron Systems, August 16–19, 1993, to be published in Physica B.
[9] R.H. Heffner, P.C. Canfield, Z. Fisk, J.D. Thompson, A. Amato, R. Feyerherm, F. Gygax, H.R. Ott, A. Schenck, D.E. MacLaughlin and J.D. Thompson, in: Proceedings of the International Conference on Strongly Correlated Electron Systems, August 16–19, 1993, to be published in Physica B.
[10] P.C. Canfield and Z. Fisk, Phil. Mag. B 65 (1992) 1117.
[11] H.C. Montgomery, J. Appl. Phys. 42 (1971) 2971.
[12] K.F. Bradley, S-H. Chen, T.O. Brun, R. Kleb, W.A. Loomis and J.M. Newsam, Nucl. Instr. Meth. A 270 (1988) 78.
[13] A.J. Freeman, in: Magnetic Properties of Rare Earth Metals, ed. R.J. Elliot (Plenum Press, New York, 1972) p. 245.
[14] D. Jerome and L.G. Caron (eds.), Low Dimensional Conductors and Superconductors (Plenum Press, New York, 1987).
[15] E. Fawcett, Rev. Mod. Phys. 60 (1988) 209.
[16] O. Eriksson, J.M. Wills and A.M. Boring, J. Alloys Compounds, in press.
[17] Recent Hall effect measurements on YbBiPt indicate that the carriers are hole-like and the carrier density is 0.05 carrier per formula unit.
[18] G.A. Gehring and K.A. Gehring, Rep. Prog. Phys. 38 (1975) 1.
[19] H.R. Ott, in: Crystalline Electric Field and Structural Effects in f-Electron Systems, eds. J.E. Crow, R.P. Guertin and T.W. Mihalisin (Plenum Press, New York, 1979).
[20] F. Hulliger, M. Landolt, H.R. Ott and R. Schmelczer, J. Low Temp. Phys. 20 (1975) 269.
[21] The anisotropy seen in Fig. 1(b) is remarkably similar to that seen in Cr below the SDW transition. See Fig. 47 of Ref. [19].
[22] T.J. Bastow and R. Street, Phys. Rev. 141 (1966) 510.
[23] Large strain sensitivity can also be inferred from temperature dependent specific heat data on pressed pellets of ground crystals. The residual strain from the grinding greatly broadens and shifts the 0.45 K anomaly. See data in Ref. [4].
[24] E.S.R. Gopal, Specific Heats at Low Temperatures (Plenum Press, New York, 1966).
[25] See Fig. 4.10 in Ref. [24].
[26] R.A. Robinson, M. Kohgi, T. Osakabe, F. Trouw, P.C. Canfield, T. Kamiyama, T. Nakane, J.D. Thompson and Z. Fisk, to be published.
[27] K.R. Lea, M.J.M. Leask and W.P. Wolf, J. Phys. Chem. Solids 23 (1962) 1381.
[28] J.E. Crow, R.P. Guertin and T.W. Mihalisin (eds.), Crystalline Electric Field and Structural Effects in f-Electron Systems (Plenum Press, New York, 1979).
[29] R.P. Guertin, W. Suski and Z. Zolnierek (eds.), Crystalline Electric Field Effects in f-Electron Magnetism (Plenum Press, New York, 1981).